Talanta 128 (2014) 242–247

Contents lists available at ScienceDirect

Talanta

journal homepage: www.elsevier.com/locate/talanta

# Intensification of the electrochemiluminescence of luminol on hollow $TiO_2$ nanoshell-modified indium tin oxide electrodes

Jia Hong [a], Liang Ming [a,b,*], Yifeng Tu [a,**]

[a] Institute of Analytical Chemistry, The Key Lab of Health Chemistry and Molecular Diagnosis of Suzhou, Soochow University, Dushu Lake Higher Education Town, Industrial Park 215123, Suzhou, PR China
[b] College of Chemistry and Chemical Engineering, Nantong University, Nantong 226019, PR China

ARTICLE INFO

*Article history:*
Received 14 February 2014
Received in revised form
28 April 2014
Accepted 2 May 2014
Available online 14 May 2014

*Keywords:*
Electrochemiluminescence
Luminol
Hollow titania nanoshells
Intensification
Hydrogen peroxide

ABSTRACT

Hollow titania nanoshells (HTNSs), which were synthesized by a $SiO_2$ sacrificial template method, were used to intensify the electrochemiluminescence (ECL) of luminol. The size, shell thickness and crystal phase, factors that are important in determining the efficiency, can be controlled by adjusting the template size, precursor concentration and calcination temperature, respectively. The structure of the HTNSs was characterized by transmission electron microscopy, scanning electron microscopy and X-ray diffraction spectroscopy. After structural optimization, the surface of indium tin oxide (ITO)-coated glass was modified with the HTNSs to act as a working electrode for a flow-injection analytical system. The heterostructure demonstrated an ECL emission intensity 150 times higher than that of the bare ITO. The research also revealed that the ECL of luminol on this modified electrode showed a very sensitive response to hydrogen peroxide with a detection limit of $4.6 \times 10^{-10}$ M. In addition to discussing the intensifying mechanism of luminol ECL by HTNSs, we demonstrate that can be successfully applied to evaluate the gross antioxidant activity of garlic.



## 1. Introduction

Electrochemiluminescence (ECL) [1] offers a number of advantages, including high sensitivity, simple instrumentation and low background noise [2,3]. It is well known that among common ECL systems consisting of inorganics, organics or semiconductors [4–8], luminol is one of the most important materials that has found widespread application. However, the fact that it requires strongly alkaline conditions and a high exciting potential severely limit its application [9,10]. In our previous work, we have proven that nanomaterials can greatly intensify the ECL of luminol [11,12] while simultaneously reducing the required pH and exciting potential.

Considerable attention has been paid to nanoscale titania (nano-$TiO_2$) in recent years because of its properties, which include high surface area, high photocatalytic activity, photovoltaic efficiency, high chemical stability and low toxicity [13–16]. It is now widely used in applications such as environmental studies, biomedicine and dye-sensitized solar cells [17–19]. Our research has revealed that nano-$TiO_2$ and related nanoscale hybrids, such as nano-$TiO_2$-supported Au atomic clusters and nano-$TiO_2$-supported AuAg alloys, show great potential for intensifying the ECL of luminol [11,20,21].

Another titania-based nanomaterial, the hollow $TiO_2$ nanoshell (HTNS), has attracted great interest for its high surface area, low density, surface permeability, good penetration and reduced charge-transport length [22–26]. It has unique properties, including multiple light diffraction, the reflection of the hollow shells [27], denser redox sites and faster charge motion than $TiO_2$ nanoparticles. For the synthesis of the HTNS, template-based or template-free strategies can be applied. Although the template-free processes involving metastable Kirkendall effect [28], Ostwald ripening [29], or chemically induced self-transformation [24,30] are relatively simple, the template-based methods have been more widely applied because of accessibility of controlled morphologies and monodispersity. Important factors can be regulated easily, such as the shape, size, shell thickness and crystal phase of the HTNS [31,32].

Our previous studies have also revealed that the ECL of luminol was intensified by reactive oxygen species (ROSs) [33], including $O_2$, hydrogen peroxide ($H_2O_2$), superoxide radicals ($O_2^{\bullet -}$), hydroxyl radicals ($^{\bullet}OH$) and $HO_2^-$. Furthermore, there are additional effects by which nanomaterials can jointly promote the ECL of luminol, which is an excellent platform for the sensitive determination of ROSs such as $H_2O_2$.

* Corresponding author at: Institute of Analytical Chemistry, The Key Lab of Health Chemistry and Molecular Diagnosis of Suzhou, Soochow University, Dushu Lake Higher Education Town, Industrial Park, 215123 Suzhou, PR China.
Tel.: +86 138 12768378; fax: +86 512 65101162.
** Corresponding author. Tel.: +86 13812768378; fax: +86 512 65101162.
*E-mail addresses:* nt_mingliang@163.com (L. Ming), tuyf@suda.edu.cn, tuyf_1@hotmail.com (Y. Tu).

http://dx.doi.org/10.1016/j.talanta.2014.05.003
0039-9140/

In this work, we have synthesized HTNSs with a $SiO_2$-sacrificial approach. The size, shell thickness and crystal structure were regulated by the template size, precursor concentration and calcination temperature, respectively. By immobilizing the HTNS onto indium tin oxide (ITO)-coated glass to act as a working electrode for flow-injection ECL (FI-ECL) detection [34,35], strong and stable luminol ECL is obtained. After optimization of the structural parameters, the ECL emission is 150 times higher than that of a bare ITO electrode. In particular, a strong and stable ECL signal was obtained under lower potential and in a nearly neutral medium. The ECL of luminol on this modified electrode is very closely related to ROSs. Thus, the gross antioxidant activity of garlic is determined for evaluation of the practicability of this modified electrode.

## 2. Experimental

### 2.1. Instruments and chemicals

A lab-built FI-ECL detection system is used as reported previously [34], which contains a flow ECL cell (approximately 5 μl of inner volume) and a six-way sample injector with a 5-μl injection loop. An RST-600 Electrochemical Workstation (custom-built, Risetest Instrument Co. Ltd., Suzhou, PR China) provided a pulsed electrolytic potential for exciting the ECL and recording it. An R212 photomultiplier tube (Hamamatsu, Japan) was used as an ECL detector (by −800 V of bias potential). A scanning electron microscope (SEM, S-4700, Hitachi, Japan) and a transmission electron microscope (TEM, FEI, USA) were used to observe the size and morphology of the nanomaterials. An X-ray diffractometer (XRD, X'PertProMPD, PANalytical B.V., Netherlands) was used to characterize the phase of the HTNSs. An Allegra 64R Centrifuge (Beckman Coulter, USA) was used to isolate the nanomaterials from the mother liquid.

ITO glass was purchased from Suzhou Nippon Sheet Glass Electronics Co., Ltd. (Suzhou, China). Luminol was purchased from Fluka (USA). Tetrabutyl titanate (TBOT, 98%), tetraethyl orthosilicate (TEOS, 99%), ethanol (99%), ammonia (26%), phosphate ($NaH_2PO_4 \cdot 2H_2O$ and $Na_2HPO_4 \cdot 12H_2O$) and NaOH were purchased from Sinopharm Chemical Reagent Co., Ltd (Shanghai, China). All of the reagents were analytical grade and used without further purification. Ultrapure water was prepared by an ALH-6000-U ultrapure water machine (Aquapro, China).

### 2.2. Preparation of the HTNS and its immobilization onto the ITO surface

Following reference [31], the HTNS was synthesized by the deposition of a $TiO_2$ shell via a sol–gel procedure onto uniformly sized $SiO_2$ templates that were prepared by the modified Stober method [36] and then etching off the $SiO_2$. A 0.1-g portion of the prepared nano-$SiO_2$ was dispersed in 33.3 ml of ethanol and TBOT was dissolved in another 33.3 ml of ethanol; these two solutions and 0.5 mL of aqueous ammonia were mixed together and vigorously stirred at 60 °C for 3 h to obtain $SiO_2$@$TiO_2$ core/shell spheres. The shell thickness was tunable by the usage of TBOT within a certain limit. A procedure of calcination of the $SiO_2$@$TiO_2$ is necessary to obtain the desired crystal phase. Afterward, the sample was etched with a NaOH solution, centrifuged and washed three times with ultrapure water. In the HTNS preparation, the parameters that strongly influence its ECL-enhancement performance, including shell size/thickness and crystal phase, were optimized.

ITO glass (1 cm × 5 cm) was cleaned in an ultrasonic bath with dilute ammonia, ethanol and ultrapure water in sequence and was dried with nitrogen flow. The HTNSs dispersed in a PVP solution were cast onto the ITO glass and sintered at 450 °C for 2 h.

### 2.3. The manipulation of the ECL measurement and important factors

For FI-ECL detection, the upper/lower limiting potential, the pulse period of the pulsed electrolytic potential and the pump flow rate are the primary factors that influence the ECL performance of luminol. In the experiments, these parameters were optimized for the best ECL performance. Thereafter, based on the intensified background ECL emission, the system responded to the injection of samples that further enhance or quench the ECL. Typically, $H_2O_2$ is a model to evaluate the performance. The detection limit, reproducibility, regression equation and linear correlation coefficient were all determined.

### 2.4. Sample preparation and detection

Under the optimized conditions, the gross antioxidant activity of garlic can be determined by the quenching effect, using resveratrol as an index (previously calibrated). A 25-g portion of the edible part of garlic flesh, purchased from local markets, was accurately weighed after peeling off the skin and was mashed with a certain volume of water in a blender. The extract was used as the sample for recovery tests and a comparative analysis (using the traditional phosphomolybdenum complex method).

## 3. Result and discussion

### 3.1. The characterization and optimization of HTNS

The structure and morphology of the HTNSs were characterized by SEM and TEM (Fig. 1). Based on the nano-$SiO_2$ templates with

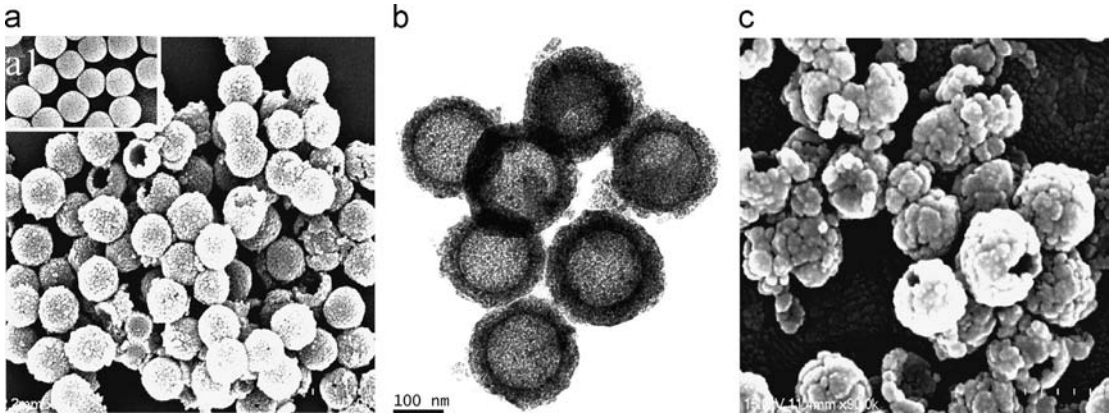


**Fig. 1.** (a) The SEM image of HTNS, here inserted (a1) is the SEM image of $SiO_2$ templates. (b) TEM image of the HTNS. (c) SEM image of calcinated HTNS under 1000 °C.

various diameters, the HTNSs were prepared with sizes of 200–500 nm by the deposition of a $TiO_2$ shell via the sol–gel procedure of the hydrolysis of TBOT. The result was a shell on the nanoscale particles (see Fig. 1A). The TEM images shown in Fig. 1B confirm the hollowing of the HTNS.

The crystalline phase of $TiO_2$ is another essential factor for the generation and migration of photogenerated electron/hole pairs whether in bulk or on a surface. It can be altered by calcination of the $SiO_2$@$TiO_2$ core/shell nanoparticles to obtain the desired phase. Fig. S1 shows the XRD patterns of the HTNSs that were obtained by calcination under various temperatures. These patterns illustrate the crystalline transformation from an amorphous phase to anatase and further to rutile, following a temperature rise from 600 °C to 1000 °C, as reported in the literature [31,32].

The calcination temperature is another important factor for the structure of the $TiO_2$ shell, as shown in Fig. 1C. A calcination temperature in excess of 900 °C will gradually destroy the shell structure due to growth of the small $TiO_2$ particles.

For the ECL of luminol on modified ITO, Fig. 2A clearly displays that smaller THNS particles led to a better working electrode and greater ECL intensification. Another important parameter that greatly affects the performance of the HTNSs is the thickness of the $TiO_2$ shell, which is tunable by varying the dosage of the precursor (TBOT). Additionally, the TBOT dosage influences the quality of the shell. Less TBOT will result in a thinner shell but might lead to defects in the shell. On the other hand, too much TBOT will cause a loss of uniformity of the HTNSs. Fig. 2B shows the optimal shell thickness of approximately 20 nm (at a TBOT dosage of 666 μL), which implies that the mesoporous hollow structure facilitates more active sites for the reactants and electron transport between the $TiO_2$ nanoparticles. Fig. 2C shows that the well-crystallized phase obtained via calcination at 800 °C enhanced the ECL the most.

Overall, the luminol ECL on the modified electrode was enhanced by 150 times compared to the ECL on a bare ITO electrode. Although the ECL strength is not equivalent to the sensitivity, the 150-fold increased ECL emission provides an excellent background for further determination.

A meaningful question is why did we not synthesize smaller HTNS to obtain a higher efficiency? As previously discussed, the $TiO_2$ shell is built with $TiO_2$ nanograins, and we can calculate approximately 400 grains (20 nm in diameter) deposited onto the surface of the $SiO_2$ template (200 nm in diameter). In contrast, we calculate only 100 grains for a template of 100 nm. Thus, it is a very difficult task to construct a smaller shell with 20-nm grains; fewer grains may not be able to build an entire shell due to the large surface curvature and surface energy.

### 3.2. ECL emission of luminol on the HTNS-modified electrode

For the best performance of the modified electrode, the dosage of HTNS or PVP was experimentally optimized. As shown in Fig. 2D, the amount of HTNS strongly affected the ECL emission of luminol on the modified electrode, and it increases with increasing dosage of HTNS until 2.0 mg. PVP is used as a dispersant and an agglomerant, and as displayed in Fig. 2E, the highest ECL emission was obtained at a PVP dosage of 9 mg/ml.

For FI-ECL analysis, the electric parameters and the buffer-solution flow rate also must be optimized [37]. Fig. 3A demonstrates the optimal flow rate of 2 ml/min. The period, the upper limiting potential and the lower limiting potential of the pulsed electrolytic potential were optimized for 3 s, 1.2 V and −0.5 V,

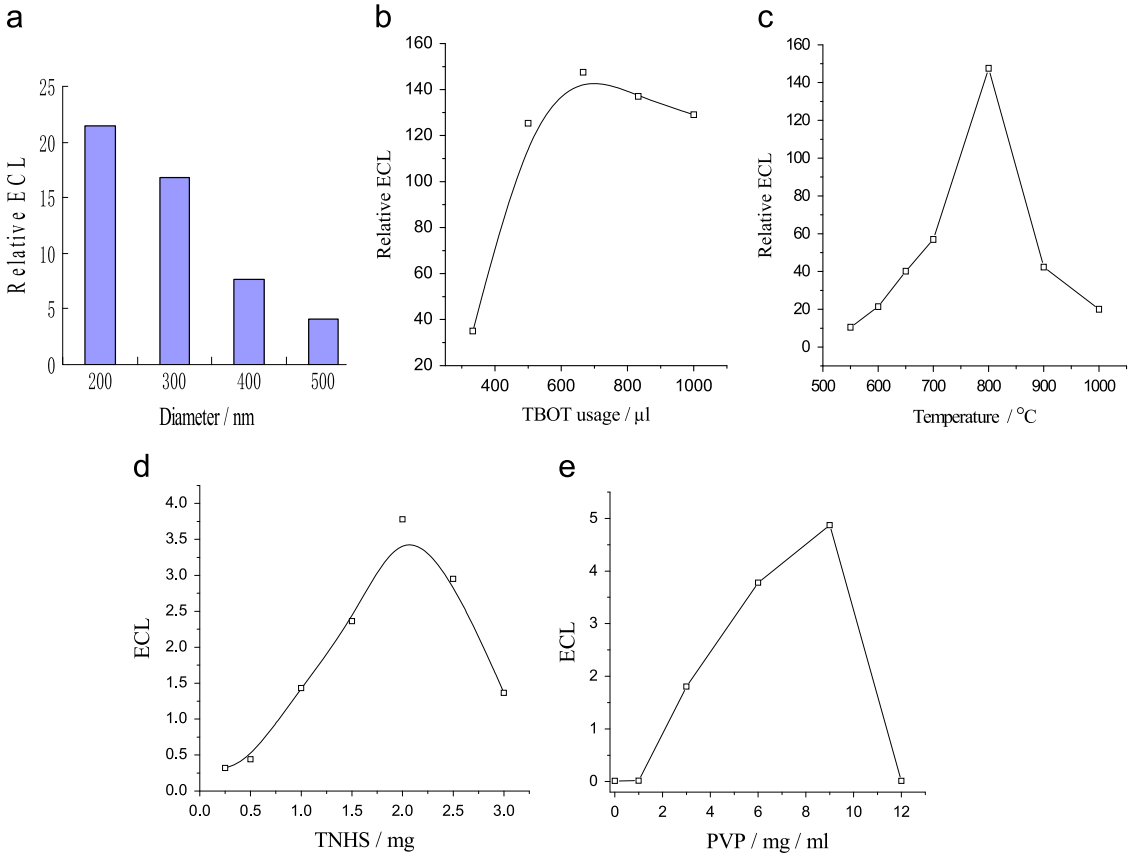


**Fig. 2.** The effect of (a) size, (b) dosage of TBOT, (c) calcination temperature, (d) the dosage of HTNS, and (e) the content of PVP on the ECL performance of the HTNS modified electrode.

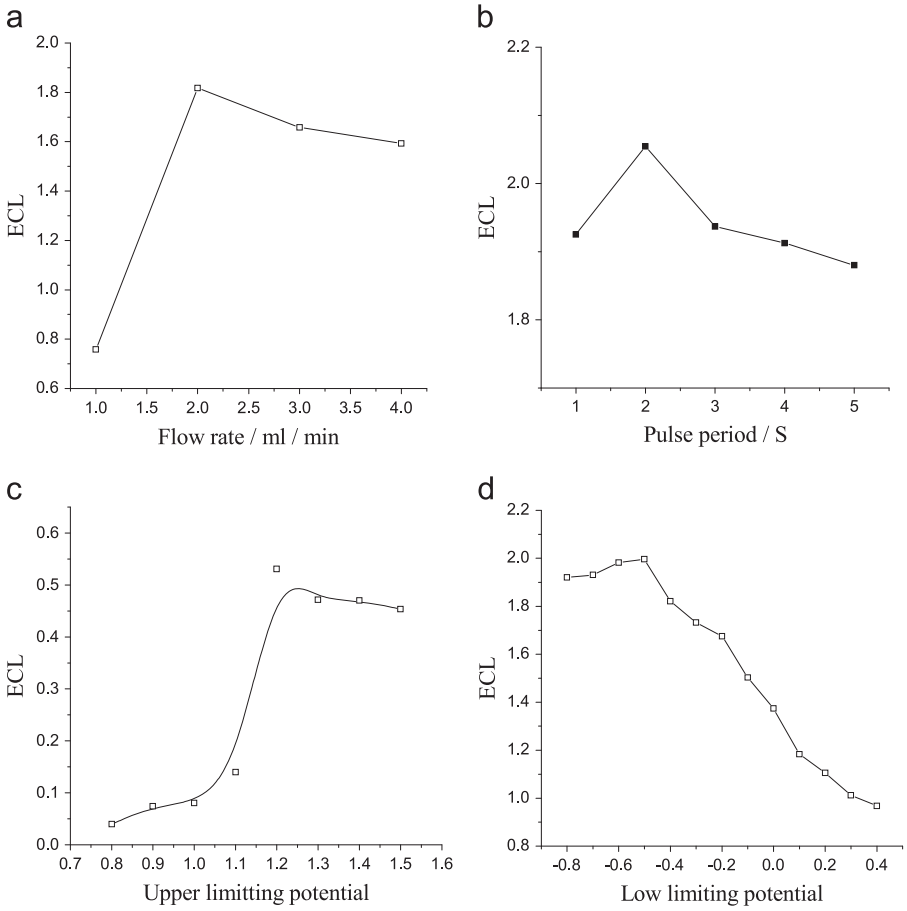


**Fig. 3.** The effect of (a) the flow rate, (b) the pulse period, (c) upper limiting potential, and (d) low limiting potential on the performance of the FI-ECL system.

**Table 1a**
Detection performance for $H_2O_2$ and resveratrol on HTNS modified electrode.

| Subject | Linear equation | Correlation coefficient | Detection limit (M) | RSD% |
|---|---|---|---|---|
| $H_2O_2$ | $\triangle$ECL=129+122C ($10^{-6}$M) | 0.999 | $4.6\times10^{-10}$ | 1.9 |
| Resveratrol | $\triangle$ECL=113+2.41C ($10^{-5}$M) | 0.996 | $2.7\times10^{-7}$ | 2.2 |

**Table 1b**
Comparison of detection limit.

| ECL systems | Detection limit (M) | Refs. |
|---|---|---|
| CdS hierarchical microspheres/GCE | $1.0\times10^{-8}$ | [38] |
| $Bi_2S_3$ nanorods/GCE, pH 10.0 | $2.0\times10^{-7}$ | [39] |
| CdTe QDs at P-GR/GCE, pH 11.0 | $9.8\times10^{-8}$ | [40] |
| CdSe nanocrystal, pH 9.3 | $1.0\times10^{-7}$ | [41] |
| Au/CdS/ITO, pH 10.0 | $5.0\times10^{-9}$ | [42] |
| $TiO_2$/ITO, luminol, pH 12.5 | $1.0\times10^{-8}$ | [43] |
| ITO, luminol, FIA, pH 9.16 | $6.0\times10^{-8}$ | [37] |
| Au/$TiO_2$/ITO, luminol, pH 8.0 | $1.58\times10^{-10}$ | [11] |
| AuAg/$TiO_2$/ITO microemulsion, FIA, pH 8.0 | $6.89\times10^{-10}$ | [21] |
| HTNS/ITO, luminol, FIA, pH 8.0 | $4.6\times10^{-10}$ | Present work |

respectively, as displayed in Fig. 3(B–D). Fig. 3C illustrates the increasing ECL intensity along with the upper limiting potential until 1.5 V, but 1.2 V is the most favorable upper limiting potential for counterbalancing the intensity and stability.

Our previous studies have revealed that ROSs are capable of intensifying the luminol ECL, and thus hydrogen peroxide can be detected as one species of the ROSs. Under the optimized conditions for this HTNS-modified electrode, the ECL emission of luminol responded linearly to the concentration of $H_2O_2$. The detection limit ($S/N=3$) for $H_2O_2$ is listed in Table 1a, which suggests that the present method is one of the most sensitive methods among those reported (see Table 1b).

Based on this foundation, this FI-ECL system may be applied to evaluate the efficiency of trace antioxidants, such as garlic, because it quenches the ECL according to its antioxidant content. Using resveratrol as the index (the quantified information is also listed in Tables 1a), the gross antioxidant activities of the three garlic samples are listed in Table 2. The recovery results are also listed

**Table 2**
Detected results of gross antioxidant in fresh garlic, the recovery and with the referential method with resveratrol as index.

| Sample | Detected result, mg/Kg, (RSD%, $n=5$) | Added | Found | Recovery, %, (RSD%, $n=5$) | With referential method, (RSD%, $n=5$) |
|---|---|---|---|---|---|
| 1 | 521(3.45) | 238<br>476<br>952 | 734<br>989<br>1526 | 89.5(2.34)<br>98.3(3.25)<br>105.6(3.84) | 494(3.26) |
| 2 | 892(3.62) | – | – | – | – |
| 3 | 2006(3.78) | – | – | – | – |

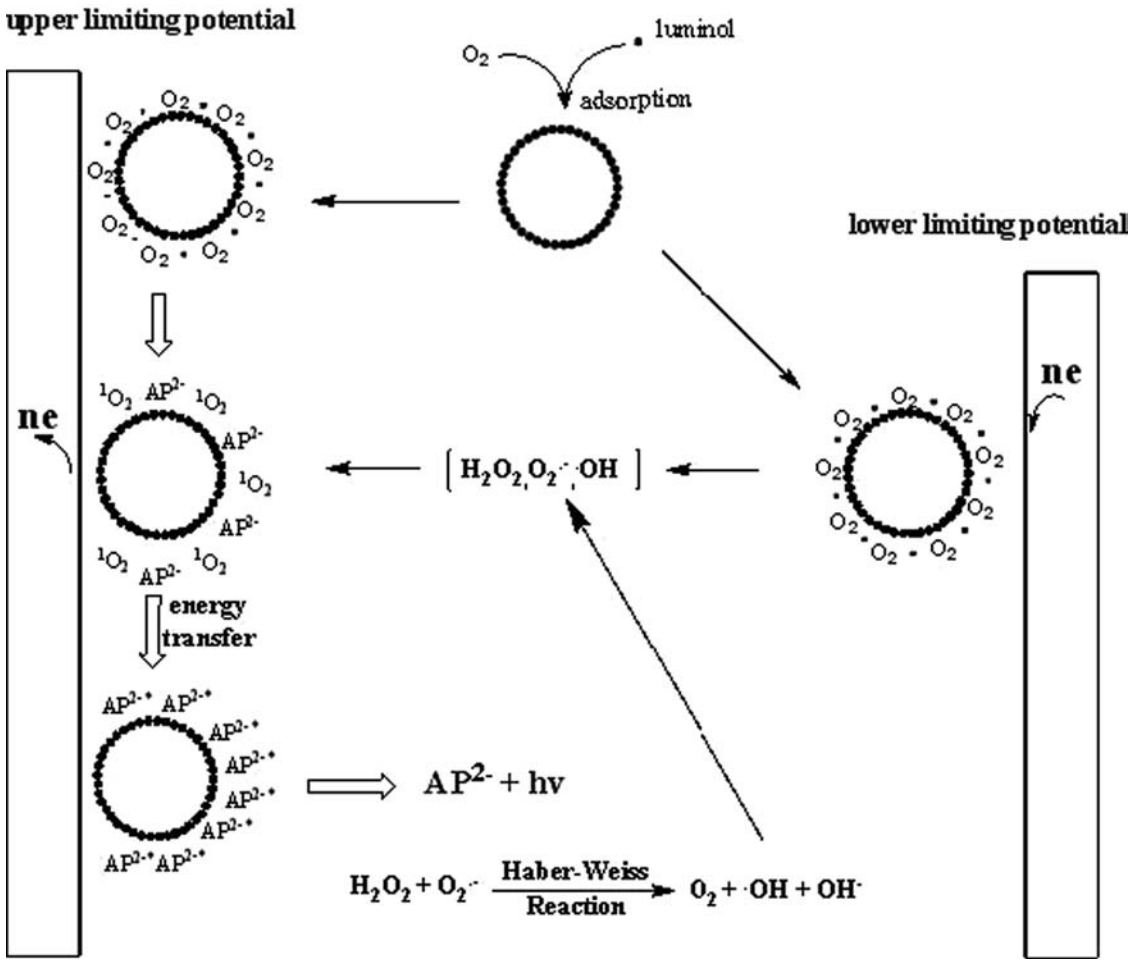


**Scheme 1.** The mechanism of enhanced ECL on the HTNS-modified electrode.

(from 89.3% to 106%). As a comparison with the phospho-molybdenum-complex method [44], we find only +5.5% of relative error.

### *3.3. The mechanism of the ECL intensification of luminol on an HTNS-modified electrode*

On the one hand, according to our previous discussion, $H_2O_2$ can be further oxidized/reduced to yield more oxidative $O_2^{\cdot-}$/$^{\bullet}$OH radicals under the upper/lower limiting potentials during the ECL process. Thus, a Haber–Weiss reaction will occur between those ROSs to yield singlet oxygen ($^1O_2$), which will further transfer the energy to the oxidized intermediate of luminol to enhance its ECL emission. On the other hand, the HTNS not only provides a larger surface area (active sites) for the electrochemical reaction of luminol and efficient electron-transport pathways, but it also enhanced the generation and migration of electron/hole pairs ($e/h^+$) [31], which promote the reduction of oxygen to yield ROSs and the oxidation of luminol to its intermediate, which transfers energy to produce stronger ECL. Scheme 1.

It can be inferred, by comparison to those titania-based nano-materials, that we have reported previously [11,21,43], the HTNS gets an equally intensifying efficiency with those hybrids of titania with nano-Au or nano-alloy; and better than the artless titania nano-particle. It implies the intrinsic merit of hollow structure that provides the properties, such as multiple reflection and diffraction [27] of light (for the as-generated ECL) in the interior of the cavity, which can induce fast migration of the electrons. It will initiate the new approach of further intensification if we got on with the hybridization of those nano-materials of noble-metals.

## 4. Conclusion

In conclusion, the HTNSs were prepared using $SiO_2$ nano-spheres as templates. The size, shell thickness and crystal phase can be controlled by the template size, precursor concentration and calcination temperature, respectively. The experimental results demonstrated that the highly crystalline HTNS with a diameter of 200 nm and a shell thickness of 20 nm possessed the greatest enhancing effect for luminol ECL of approximately 150 times when it was immobilized onto the surface of ITO. The ECL of luminol on this modified electrode showed a very sensitive response to hydrogen peroxide; thus, it was applied to evaluate the gross antioxidant efficiency of samples such as garlic. This approach represents significant progress toward the development of a new approach to monitor the oxidative stress in human diseases and disorders.

## Acknowledgments

This work is supported by the National Natural Science Foundation of China (21175096, 21375091) and the Project of Scientific and Technologic Infrastructure of Suzhou (SZS201207).

## Appendix A. Supplementary materials

Supplementary data associated with this article can be found in the online version at http://dx.doi.org/10.1016/j.talanta.2014.05.003.

## References


[1] M.M. Richter, Chem. Rev. 104 (2004) 3003–3036.
[2] W.J. Miao, Chem. Rev. 108 (2008) 2506–2553.
[3] K.A. Fähnrich, M. Pravda, G.G. Guilbault, Talanta 54 (2001) 531–559.
[4] R.Y. Lai, A.J. Bard, J. Phys. Chem. A 107 (2003) 3335–3340.
[5] A. Wróblewska, O.V. Reshetnyak, E.P. Koval'chuk, R.I. Pasichnyuk, J. Błażejowski, J. Electroanal. Chem. 580 (2005) 41–49.
[6] B.A. Gorman, P.S. Francis, N.W. Barnett, Analyst 131 (2006) 616–639.
[7] A.J. Bard, Z.F. Ding, N. Myung, Struct. Bonding (Berlin. Germany) 118 (2005) 1–57.
[8] L. Dennany, M. Gerlach, S. O'Carroll, T.E. Keyes, R.J. Forster, P. Bertoncello, J. Mater. Chem. 21 (2011) 13984–13990.
[9] C.A. Marquette, L.J. Blum, Sens. Actuators, B 90 (2003) 112–117.
[10] J. Suomi, M. Håkansson, Q.H. Jiang, M. Kotiranta, M. Helin, A.J. Niskanen, S. Kulmala, Anal. Chim. Acta 541 (2005) 167–169.
[11] Z.M. Yu, X.H. Wei, J.L. Yan, Y.F. Tu, Analyst 137 (2012) 1922–1929.
[12] X.H. Wei, C.B. Xiao, K. Wang, Y.F. Tu, J. Electroanal. Chem. 702 (2013) 37–44.
[13] U. Bach, D. Lupo, P. Comte, J.E. Moser, F. Weissortel, J. Salbeck, H. Spreitzer, M. Grätzel, Nature 395 (1998) 583–585.
[14] M. Grfitzeli B. O'regan, Nature 353 (1991) 737–740.
[15] A.L. Linsebigler, G.Q. Lu, J.T. Yates Jr, Chem. Rev. 95 (1995) 735–758.
[16] R. Nakamura, N. Ohashi, A. Imanishi, T. Osawa, Y. Matsumoto, H. Koinuma, Y. Nakato, J. Phys. Chem. B 109 (2005) 1648–1651.
[17] C. Vitale-Brovarone, G. Novajra, D. Milanese, J. Lousteau, J.C. Knowles, Mater. Sci. Eng. C 31 (2011) 434–442.
[18] Z.P. Xing, J.Z. Li, Q. Wang, W. Zhou, G.H. Tian, K. Pan, C.G. Tian, J.L. Zou, H.G. Fu, Eur. J. Inorg. Chem. 2013 (2013) 2411–2417.
[19] Z.Q. Sun, J.H. Kim, Y. Zhao, D. Attard, S.X. Dou, Chem. Commun. 49 (2013) 966–968.
[20] K. Wang, X.H. Wei, Y.F. Tu, Microchim. Acta (2014), http://dx.doi.org/10.1007/s00604-014-1224-7.
[21] X.H. Wei, C. Xiao, C. Liu, K. Wang, Y.F. Tu, Electroanalysis (2014), http://dx.doi.org/10.1002/elan.201300559.
[22] S.C. Lee, C.W. Lee, J.S. Lee, Mater. Lett. 62 (2008) 564–566.
[23] Y. Kondo, H. Yoshikawa, K. Awaga, M. Murayama, T. Mori, K. Sunada, S. Bandow, S. Iijima, Langmuir 24 (2008) 547–550.
[24] J.G. Yu, J. Zhang, Dalton Trans. 39 (2010) 5860–5867.
[25] A. Syoufian, O.H. Satriya, K. Nakashima, Catal. Commun. 8 (2007) 755–759.
[26] A. Syoufian, K. Nakashima, J. Colloid Interface Sci. 313 (2007) 213–218.
[27] H.X. Li, Z.F. Bian, J. Zhu, D.Q. Zhang, G.S. Li, Y.N. Huo, H. Li, Y.F. Lu, J. Am. Chem. Soc. 129 (2007) 8406–8407.
[28] Y.W. Wang, H. Xu, X.B. Wang, X. Zhang, H.M. Jia, L.Z. Zhang, J.R. Qiu, J. Phys. Chem. B 110 (2006) 13835–13840.
[29] H.G. Yang, H.C. Zeng, J. Phys. Chem. B 108 (2004) 3492–3495.
[30] J.G. Yu, H. Guo, S.A. Davis, S. Mann, Adv. Funct.Mater. 16 (2006) 2035–2041.
[31] H.L. Shen, H.H. Hu, D.Y. Liang, H.L. Meng, P.G. Li, W.H. Tang, C. Cui, J. Alloys Compd. 542 (2012) 32–36.
[32] J.B. Joo, Q. Zhang, I. Lee, M. Dahl, F. Zaera, Y.D. Yin, Adv. Funct. Mater. 22 (2012) 166–174.
[33] H.H. Chu, W.Y. Guo, J.W. Di, Y. Wu, Y.F. Tu, Electroanalysis 21 (2009) 1630–1635.
[34] C. Liu, X.H. Wei, Y.F. Tu, Talanta 111 (2013) 156–162.
[35] X.H. Wei, C. Liu, Y.F. Tu, Talanta 94 (2012) 289–294.
[36] H.L. Meng, C. Cui, H.L. Shen, D.Y. Liang, Y.Z. Xue, P.G. Li, W.H. Tang, J. Alloys Compd. 527 (2012) 30–35.
[37] M. Chen, X.H. Wei, Y.F. Tu, Talanta 85 (2011) 1304–1309.
[38] Y.H. Xu, C.X. Song, Y.W. Sun, D.B. Wang, Mater. Lett. 65 (2011) 1762–1764.
[39] Y.P. Dong, L.Z. Pei, X.F. Chu, W.B. Zhang, Q.F. Zhang, Analyst 138 (2013) 2386–2391.
[40] Z.H. Wang, H.J. Song, H.H. Zhao, Y. Lv, Luminescence 28 (2013) 259–264.
[41] G.Z. Zou, H.X. Ju, Anal. Chem. 76 (2004) 6871–6876.
[42] C.G. Shi, Y. Shan, J.J. Xu, H.Y. Chen, Electrochim. Acta 55 (2010) 8268–8272.
[43] W.Y. Guo, J.L. Yan, Y.F. Tu, Sci. China: Chem. 54 (2011) 1640–1644.
[44] R. Mohamed, M. Pienda, M. Aguilar, J. Food Sci. 72 (2007) S059–S063.